



ISOLATION OF NUCLEAR CONTAINMENT VESSELS CONSIDERING FLUID-STRUCTURE INTERACTION

Joshua A. Hoekstra¹, Tracy C. Becker², Michael J. Tait³

¹ Graduate Student, CaNRisk-CREATE, Department of Civil Engineering, McMaster University, Hamilton, ON, Canada (hoekstja@mcmaster.ca)

² Assistant Professor, Department of Civil and Environmental Engineering, University of California Berkeley, Berkeley, CA, USA

³ Department Chair, Department of Civil Engineering, McMaster University Hamilton, ON, Canada

ABSTRACT

The safe operation and structural integrity of nuclear power plants must be ensured in the event of severe loading conditions, such as earthquakes. Structurally, seismic isolation is a common method used to reduce damage; however, its use amongst nuclear structures is limited. A common safety feature in certain Generation III+ nuclear reactors is a passive containment cooling tank, located at the top of the structure. The mass of water in such tanks is significant and should be considered in the analysis of the containment structure. Nuclear containment vessels have been modelled to account for fluid-structure interaction, but this has been focused on fixed-base structures. Isolation has been proven to be beneficial for nuclear power plants; however, these studies have not included fluid tank behaviour. It has been observed that in isolated liquid storage tanks, engineering responses including base shear, overturning moment, and peak hydrodynamic pressure are reduced at the expense of increased sloshing displacements which could be of concern in nuclear power plants. This study models an isolated nuclear containment vessel, considering fluid-structure interaction from the cooling tank, to understand how fluid sloshing influences the response of an isolated nuclear containment vessel under seismic loading. It is found that isolation reduces the peak hydrodynamic force, and that peak floor acceleration and drift can be increased due to fluid-structure interaction

INTRODUCTION

Nuclear Power Plants (NPPs) are critical infrastructure and must be designed so that the probability of failure is very low, as the repercussions are dire. A common feature of Generation III+ NPPs is the incorporation of a large passive cooling tank, located at the top of the structure. Under dynamic excitation, the fluid in these tanks may slosh, which can impact the behaviour of the structure. Previous studies have investigated sloshing fluid in NPPs. Song et al. (2017) compared the use of a finite element fluid model to a linear equivalent mechanical sloshing model in a NPP and found that the linear equivalent mechanical model had excellent agreement with the finite element model in terms of sloshing frequencies and fluid shear force generated against the tank. Studies have shown that when compared to a model with an empty tank, considering fluid-structure interaction (FSI) can lead to increased (Zhao, Chen, and Xu, 2014) or decreased (Xu et al., 2016) acceleration responses of the containment structure, depending on the fluid level in the tank. Additionally, floor response spectra (FRS) is influenced by FSI, which led to a recommendation to include FSI in design considerations (Song et al., 2017). For a reactor vessel with an irregular toroidal shaped tank with an elliptical bottom, Sviatoslavsky et al. (2013) found that multiple sloshing modes should be considered when using an equivalent mechanical model to accurately estimate sloshing displacement. In all of these cases, the NPPs were of conventional, fixed-base construction.

The effectiveness of base isolation in reducing seismic demands on structures is well established; however, its use in the nuclear industry is limited (Naeim and Kelly, 1999). Chen et al. (2014) demonstrated that structural drift and acceleration can be significantly reduced in a Generation III+ NPP by employing base isolation. Base isolation has also been shown to reduce FRS values in nuclear facilities (Whittaker et al., 2008), which is important as they house expensive and safety-critical non-structural components. Huang et al. (2007) and Whittaker et al. (2008) analyzed several base isolation models for suites of ground motions and found isolation effective in every instance when compared to fixed base nuclear facilities, however, FSI was not considered in the model of the NPP.

The combination of isolation and FSI has been studied, but not for NPPs. Liquid storage tanks have been isolated, with investigations on their behavior focusing on structural demands to the tank. Saha et al. (2014) investigated base isolated broad and slender liquid storage tanks subject to ground motions using an equivalent mechanical sloshing model, and found that the base shear and overturning moment of the tank were mainly attributed to the impulsive mass of fluid and that isolation systems with low yield displacements reduced responses more than those with high yield displacements. Shrimali and Jangid (2002) used an equivalent mechanical sloshing model for an isolated liquid storage tank and suggested that an optimum value for isolation yield strength exists for which base shear is minimized. They also found that slosh heights were increased for the isolated model. Moslemi and Kianoush (2016) looked at an isolated, elevated liquid storage tank and recommended that the isolation period be well separated from the sloshing period to avoid resonance. They also found that even though isolation reduced the seismic demands on the tower, it increased sloshing displacements.

This paper will investigate the effects of FSI on fixed base and base isolated NPPs. A lumped mass–stick model is used for the NPP, and a linear equivalent mechanical model is used for the fluid in the tank, while a bilinear model will be used for the isolation system. To investigate the effects of sloshing in a nuclear reactor, sloshing heights and the lateral fluid force against the tank will be compared for fixed base and isolated cases, as this has not been the focus of previous studies. Additionally, the responses of an isolated reactor with an empty tank will be compared to the responses of an isolated reactor with fluid sloshing, and an isolated reactor with all fluid treated as rigid to investigate the impact of FSI on the responses of an isolated NPP reactor.

MODEL DESCRIPTION

Sample Reactor Model

The lumped mass–stick idealization of the sample NPP reactor is provided in Figure 1. The two lumped mass–stick models represent the containment vessel (CV), which is the protective shell component of the reactor and the internal structure (IS), which is where the reactor and related non-structural components are housed. The CV and IS are joined at the base but are otherwise structurally independent. Additional information about the model can be found in Whittaker et al. (2008), as the model used in this study is similar; however, the analysis done in this study is in-plane. Additionally, for two of the models the mass at the node of the CV representing the tank is altered to account for the fluid in the tank, as the original model treated the entire fluid mass as rigid at that point. Both the CV and IS are assumed to remain elastic. The properties of the CV and the IS are summarized in Table 1.

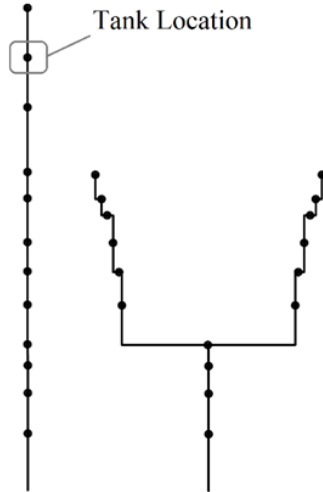


Figure 1: Representative nuclear reactor CV (left) and IS (right) stick models

Table 1: Model properties

	Containment Vessel	Internal Structure
Height (m)	59.5	39
Mass (tonne)	20936 ¹ , 22770 ² , 25034 ³	23835
Fundamental Period (s)	0.175 ¹ , 0.186 ² , 0.215 ³	0.129
Water Mass (tonne)	4098	0

¹ Model with empty tank

² Model with equivalent mechanical rigid fluid mass (excludes sloshing masses)

³ Model with total fluid mass treated as rigid

The isolation system was designed for the hazard associated with the Diablo Canyon NPP site. The United States Nuclear Regulatory Commission (USNRC) recommends that nuclear facilities be seismically designed using a uniform hazard spectrum (UHS) with mean annual frequency of exceedance (MAFE) of 1×10^{-4} to generate a uniform reliability spectrum (URS) with more stringent standards than the UHS (McGuire et al., 2001). Similar provisions exist in Canada, where the design spectrum is created for mean probability of exceedance of 1×10^{-4} or lower (Canadian Standards Association, 2015). The base isolation system is modelled using a bilinear hysteresis which represents a friction pendulum system with a second stiffness period of 4.4 s, yield displacement of 1 mm, and post-yield stiffness ratio of 0.0052. The isolation system has a design displacement of 600mm, so as not to exceed the displacement limit of flexible pipe connections to the reactor structure, which is taken as 900mm (Forni et al., 2014). In the base isolated model, the CV and IS are mounted on a single isolation mat, which has a mass of 26367 tonnes.

Sloshing Fluid Model

The water in the cooling tank is modelled using a linear equivalent mechanical system. The equivalent mechanical system is established by dividing the fluid into two components: a rigid component that moves with the tank and a convective component that oscillates separately (Ibrahim, 2005). The convective component represents the sloshing modes, of which only the asymmetric modes contribute to the net lateral force produced by the fluid sloshing on the tank. The equivalent mechanical model is displayed in Figure 2, where m_n , c_n , and k_n represent the mass, damping and stiffness respectively of the n^{th} sloshing mode. The rigid mass component, m_o , is added directly to the lumped mass of the CV at the location of the tank, while the three sloshing masses considered are attached to that same degree of freedom using springs and

dashpots. The equivalent mechanical model assumes that the fluid motion remains approximately linear during analysis.

The frequency, mass, stiffness, and damping of the equivalent mechanical system depend on the shape of the tank. For the NPP considered, the tank is an upright cylinder with an annular cross-section and sloped exterior walls. When the tank is filled to its design water depth, the volume of water is 4098 m³, with about 1 m of freeboard. Tanks with irregular geometry are often idealized using a tank with regular geometry and equivalent volume. Mesarole and Fortini (1987) modelled a toroidal tank by using an equivalent annular tank that had the same volume. Song et al. (2017) modelled an annular tank with a sloped base as an equivalent annular tank with a flat base by equating the volumes of each tank, and found the equivalent annular tank represented the actual tank well. Thus, in this study, the annular NPP tank with sloped walls is idealized as an equivalent annular tank with vertical walls that has the same volume as the NPP tank. The outer radius of the equivalent tank was altered to equate the volumes. The properties of the equivalent mechanical system are summarized in Table 2.

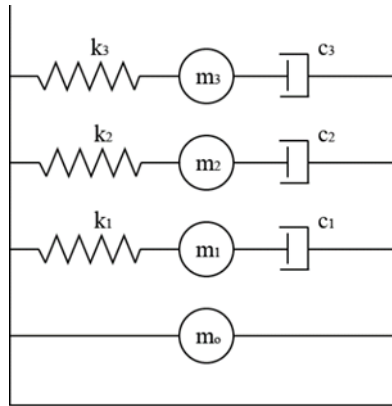


Figure 2: Equivalent mechanical fluid model

The frequencies of the asymmetric sloshing modes (ω_{1n}) ($n = 1, 2, 3 \dots$) are calculated using (Ibrahim, 2005):

$$\omega_{1n}^2 = \frac{\xi_{1n}g}{R_o} \tanh\left(\frac{\xi_{1n}h}{R_o}\right) \quad (1)$$

Where g is the acceleration due to gravity, R_o is the outer radius of the equivalent annular tank, h is the fluid height in the equivalent annular tank, and ξ_{1n} are the n^{th} roots of Equation 2:

$$J'_1(\xi)Y'_1(k\xi) - J'_1(k\xi)Y'_1(\xi) = 0 \quad (2)$$

In which k is the ratio of inner to outer radius, J'_1 and Y'_1 are Bessel Functions of the first and second kind, respectively, and the prime denotes the derivative with respect to ξ . The equivalent mechanical sloshing masses are determined using the methods outlined by Bauer (1961).

The peak height of the sloshing fluid (h_s) when considering the effect of horizontal base excitation only for a cylindrical tank is estimated by (Bandyopadhyay et al., 1995):

$$h_s = R_o \sqrt{\left(\frac{0.837(S_a)_1}{g}\right)^2 + \left(\frac{0.073(S_a)_2}{g}\right)^2 + \left(\frac{0.028(S_a)_3}{g}\right)^2} \quad (3)$$

Where $(S_a)_n$ ($n = 1,2,3$) is the spectral acceleration of sloshing mode n . Bandyopadhyay et al. (1995) showed that if the first three sloshing modes are considered, more accurate estimates of sloshing height can be made for a cylindrical tank.

Table 2: Equivalent mechanical system properties

Sloshing Mode	Period (s)	Mass (tonne)	Percentage of Water Mass
1	7.413	2762	67.4%
2	3.506	232	5.7%
3	2.710	18	0.4%
Rigid Fluid		1087	26.5%

ANALYSIS

To cover a variety of earthquake characteristics, dynamic analysis was conducted using 11 shallow crustal earthquake ground motions, characteristic of the hazard at a west coast US location. The 11 ground motions used for analysis were scaled to the UHS with MAFE of 1×10^{-4} for the Diablo Canyon NPP site in California. The scaled acceleration response spectra for the suite of ground motions is shown in Figure 3. Analysis was run using MATLAB for four model cases, which are outlined in Table 3. Comparing the results of Models 1 and 2 provides insight as to how base isolation influences the sloshing behaviour of the tank, while comparing the results of Models 2, 3 and 4 illustrates how FSI impacts structural responses of the NPP reactor.

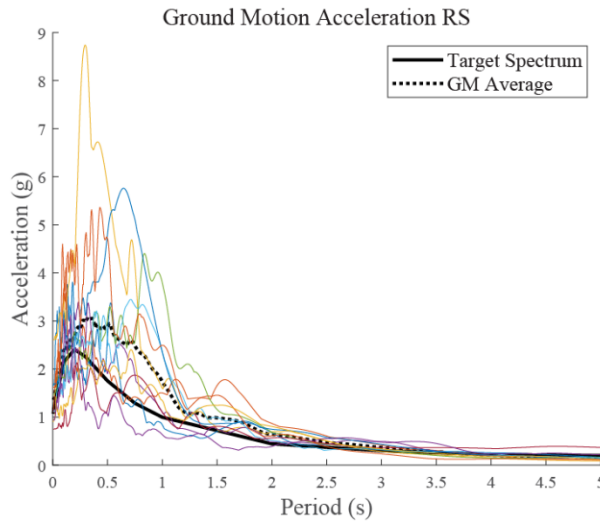


Figure 3: Spectral accelerations for ground motions

Table 3: Model cases

Model Case	Base Behaviour	Tank Behaviour
Model 1	Fixed Base	Sloshing Fluid
Model 2	Base Isolated	Sloshing Fluid
Model 3	Base Isolated	Empty
Model 4	Base Isolated	Rigid Fluid

RESULTS AND DISCUSSION

Figure 4 compares the response of the isolated and fixed base models both with sloshing tanks. It is seen that isolating the reactor structure can increase or decrease peak fluid sloshing height, depending on the ground motion. As shown in Table 2, the period of the first sloshing mode (7.413s) is well separated from the effective isolation period, which is 3.3s on average for the suite of ground motions. The second (3.506s) and third (2.710s) fluid sloshing modes have natural periods much closer to the effective isolation period and would be excited more intensely than the first. However, the overall contribution from the second and third sloshing mode to peak sloshing height is minor compared to the fundamental sloshing mode, which limits the change in peak sloshing height. For earthquakes 5, 6, and 7, both the isolated and fixed base models have sloshing displacements greater than 1 m. These slosh heights exceed the freeboard of the tank, so in these cases, fluid impact with the roof would have to be accounted for to produce more accurate results.

The tank shear is measured as the force produced by the sum of the convective and rigid fluid components. For all eleven ground motions, the implementation of base isolation decreases tank shear. Most of the reduction in tank shear is due to the decrease in acceleration of the rigid fluid component, which experiences the same reduction in acceleration as the containment vessel when it is base isolated. Unlike the rigid component of fluid, the convective component does not experience a consistent reduction in force, as three of the eleven earthquakes caused an increase in convective shear. Despite this, the net tank shear is consistently reduced because the impulsive fluid component accounts for a much greater percentage of the tank shear force than the convective fluid component. As shown in Table 2, the fundamental fluid sloshing mode accounts for most of the mass participation of the convective portion of the fluid. Since its natural period is well separated from the effective isolation period, the use of base isolation does not cause it to appreciably come into resonance with the isolation system.

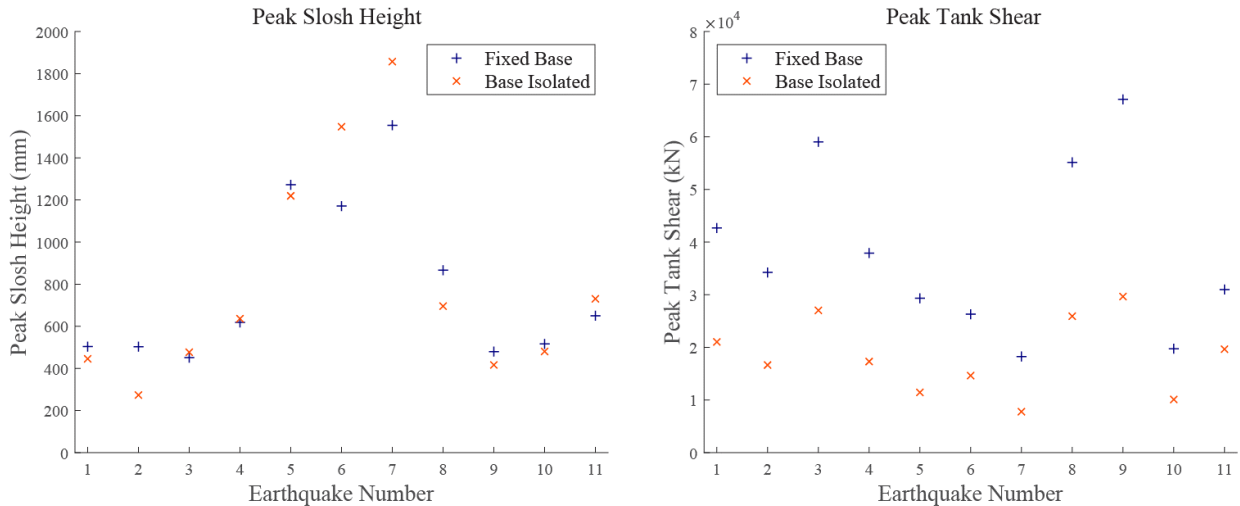


Figure 4: Peak slosh heights and tank shears for Models 1 (fixed base) and 2 (base isolated)

Figure 5 compares the acceleration, drift and base shear responses of the base isolated models with and without the tank filled. There is no clear pattern with regards to how sloshing fluid affects the peak floor acceleration at the location of the tank. For five earthquakes the model with an empty tank had larger peak acceleration, while for three earthquakes the sloshing tank had greater results and for the three other earthquakes, both models produced similar results. As such, it cannot be concluded that fluid-structure interaction decreases acceleration at the location of the tank when the structure is subject to an earthquake, but FSI should be accounted for in design as it may yield higher peak floor accelerations than if it was neglected.

The influence of fluid-structure interaction on peak roof drift is more consistent, as for seven of the eleven earthquakes, peak roof drift is increased when FSI is considered. Roof drift is measured as the difference in displacement between the top and base of the CV, that is, relative to the isolation system. The rigid component of the fluid in Model 2 increases the mass of the containment vessel, which in turn marginally increases the fundamental period of the CV (see Table 1), so it is expected that displacement should also be marginally increased. For most cases, the effects of the convective components of fluid sloshing are not large enough to significantly alter structural drift. However, for two earthquakes, the peak drift of the sloshing tank model is less than that of the empty tank model, which demonstrates that FSI can result in reduced drift for select ground motions, but not in general.

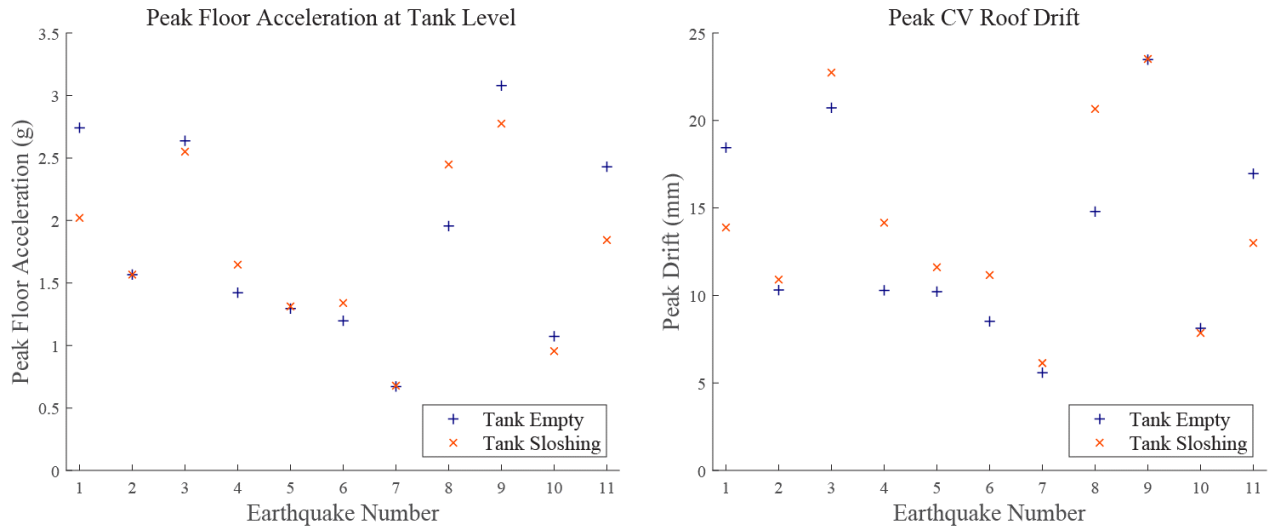


Figure 5: Peak floor acceleration and drift for Models 2 (sloshing) and 3 (empty)

To observe the effects of purely adding mass to the system, peak acceleration and drift were plotted for the height of the CV, as depicted in Figure 6. The results shown are for earthquake 8, the ground motion that produced the median peak tank shear.

Of the three models, the rigid fluid model has the heaviest containment vessel, as all fluid mass is rigidly attached to the CV. The mass of the sloshing fluid model's CV is marginally greater than the empty tank model, and less than the rigid fluid model as only a portion of the fluid mass is rigidly attached to the CV. The rigid fluid model exhibits the lowest peak acceleration, which is expected as it has the longest fundamental period of the three models. The peak drift of the rigid fluid model is also higher than the empty tank model, which is also expected as a result of its longer fundamental period. The sloshing fluid model exhibits drifts that are higher than both the empty tank model and the rigid fluid model. Additionally, the peak acceleration of the sloshing fluid model is higher than both other models for the top half of the structure. These results are not consistent with an explanation based purely on fundamental period, and must be attributed to the effects of fluid-structure interaction on the CV. In this case, FSI should be

considered in design models as the sloshing fluid model produces the largest peak floor accelerations and peak drifts.

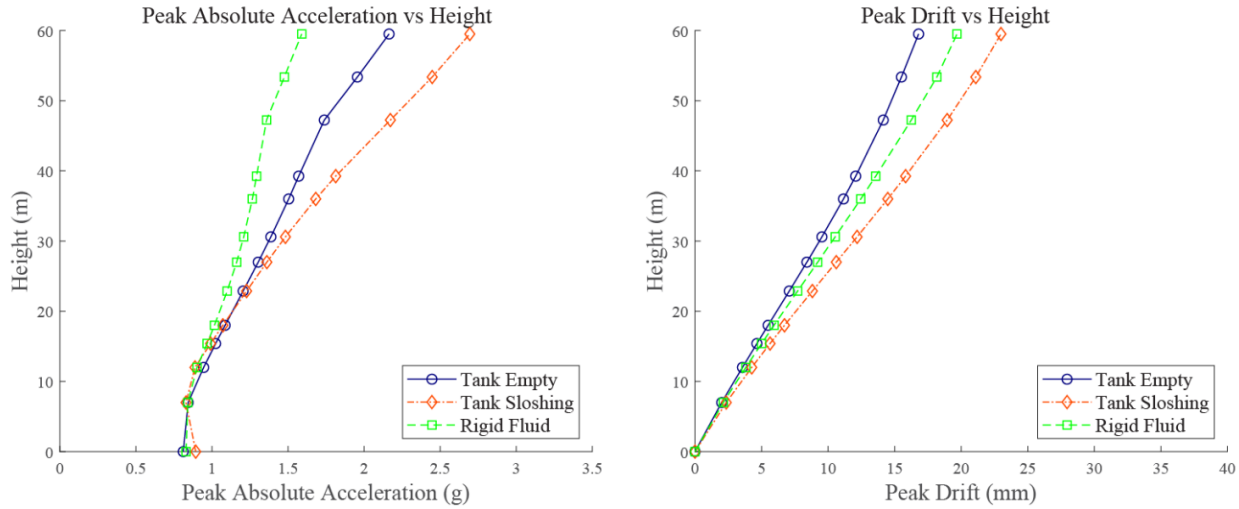


Figure 6: Peak acceleration and drift for each storey for Models 2 (sloshing), 3 (empty) and 4 (rigid)

CONCLUSIONS

The effects of FSI on seismic responses of an NPP reactor were investigated using four lumped mass–stick models, representing the cases of a fixed base reactor with fluid sloshing, isolated reactor with fluid sloshing, isolated reactor with an empty tank, and isolated reactor with rigid fluid.

In general, isolation reduces peak shear force of the water tank. Peak sloshing heights can be increased or decreased due to isolation, depending on the ground motion, and should be modelled as they have the potential to exceed the freeboard of the tank.

For an isolated reactor model, the effects of FSI on peak floor acceleration are not consistent. In some cases, peak floor acceleration is increased when the model includes FSI, which suggests that FSI should be accounted for when designing acceleration-sensitive components. The effects of FSI on peak drift are more constant; the added mass due to water increases drift, while the convective action of the fluid may have an impact. Using a rigid fluid model cannot necessarily capture the effects of FSI on peak floor acceleration or drift conservatively. As such, FSI should be considered in the analysis of a NPP reactor with a large passive cooling tank, as it will impact the seismic response of the structure.

ACKNOWLEDGEMENTS

The financial support for the study was provided through the Canadian Nuclear Energy Infrastructure Resilience under Systemic Risk (CaNRisk) – Collaborative Research and Training Experience (CREATE) program of the Natural Science and Engineering Research Council (NSERC) of Canada.

REFERENCES

- Bandyopadhyay, K., Cornell, A., Costantino, C., Kennedy, R., Miller, C., & Veletsos, A. (1995). "Seismic Design and Evaluation Guidelines for the Department of Energy High-Level Waste Storage Tanks and Appurtenances." Engineering Research and Applications Division, Department of Advanced Technology, Brookhaven National Laboratory, Upton, New York.
- Bauer, H.F. (1961). "Mechanical analogy of fluid oscillations in cylindrical tanks with circular and annular cross-section." MSFC, NASA, MTP-AERO61-4.
- Chen, J., Zhao, C., Xu, Q., & Yuan, C. (2014). "Seismic analysis and evaluation of the base isolation system in AP1000 NI under SSE loading." *Nuclear Engineering and Design*, 278, 117–133.
- Canadian Standards Association (CSA). (2015). "Design procedures for seismic qualification of nuclear power plants." *CSA N289.3-10*, Mississauga, Canada
- Forni, M., Poggianti, A., Scipinotti, R., Dusi, A., & Manzoni, E. (2014). "Seismic isolation of lead-cooled reactors: The European project SILER." *Nuclear Engineering and Technology*, 46(5), 595–604.
- Huang, Y. N., Whittaker, A. S., Constantinou, M. C., & Malusht, S. (2007). "Seismic demands on secondary systems in base-isolated nuclear power plants." *Earthquake Engineering and Structural Dynamics*, 36(12), 1741–1761.
- Ibrahim, R.A. (2005). *Liquid Sloshing Dynamics - Theory and Applications*, Cambridge University Press, New York.
- McGuire, R.K., Silva, W.J., & Costantino, C.J. (2001). "Technical Basis for Revision of Regulatory Guidance on Design Ground Motions: Hazard- and Risk-consistent Ground Motion Spectra Guidelines.", *NUREG/CR-6728*, Division of Engineering Technology, U.S. Nuclear Regulatory Commission, Washington, D.C.
- Meserole, J. S., & Fortini, A. (1987). "Slosh dynamics in a toroidal tank." *Journal of Spacecraft and Rockets*, 24(6), 523–531.
- Moslemi, M., & Kianoush, M. R. (2016). "Application of seismic isolation technique to partially filled conical elevated tanks." *Engineering Structures*, 127, 663–675.
- Naeim, F., & Kelly, J. M. (1999). *Design of Seismic Isolated Structures: From Theory to Practice*, Wiley, New York.
- Saha, S. K., Matsagar, V. A., & Jain, A. K. (2014). "Earthquake Response of Base-Isolated Liquid Storage Tanks for Different Isolator Models." *Journal of Earthquake and Tsunami*, 08(05), 1450013.
- Shrimali, M. K., & Jangid, R. S. (2002). "Non-linear seismic response of base-isolated liquid storage tanks to bi-directional excitation." *Nuclear Engineering and Design*, 217(1–2), 1–20.
- Song, C., Li, X., Zhou, G., & Wei, C. (2017). "Research on FSI effect and simplified method of PCS water tank of nuclear island building under earthquake." *Progress in Nuclear Energy*, 100(September 2017), 48–59.
- Sviatoslavsky, G., Prakash, A., Demitz, J., Vieira, A., & Reifschneider, M. (2013). "Sloshing in a Large Water Tank of a Non-standard Configuration Subjected to Seismic Loading." *Transactions, 22nd Conference on Structural Mechanics in Reactor Technology (SMiRT-22)*, San Francisco, CA.
- Whittaker, A., Huang, Y.-N., & Luco, N. (2008). "Performance Assessment of Conventional and Base-Isolated Nuclear Power Plants for Earthquake and Blast Loadings." *MCEER-08-0019*, Multidisciplinary Center for Earthquake Engineering Research, University at Buffalo, The State University of New York, Buffalo, NY.
- Xu, Q., Chen, J., Zhang, C., Li, J., & Zhao, C. (2016). "Dynamic Analysis of AP1000 Shield Building Considering Fluid and Structure Interaction Effects." *Nuclear Engineering and Technology*, 48(1), 246–258.
- Zhao, C., Chen, J., & Xu, Q. (2014). "FSI effects and seismic performance evaluation of water storage tank of AP1000 subjected to earthquake loading." *Nuclear Engineering and Design*, 280(August), 372–388.